NBSIR 76-1078

Piezoelectric Polymer Transducers for Dynamic Pressure Measurements

Aime S. DeReggi, Seymour Edelman, and Steven C. Roth

Institute for Materials Research
National Bureau of Standards
Washington, D. C. 20234

June 1976

Final

NBSIR 76-1078

PIEZOELECTRIC POLYMER TRANSDUCERS FOR DYNAMIC PRESSURE MEASUREMENTS

Aime S. DeReggi, Seymour Edelman, and Steven C. Roth

Institute for Materials Research
National Bureau of Standards
Washington, D. C. 20234

June 1976

Final

Introduction

This report covers work completed on December 31, 1975, on thin (approximately 50 μm or 0.002 in. thick) piezoelectric polymer transducers which were developed at the National Bureau of Standards (NBS) for the National Highway Traffic Safety Administration (NHTSA) for use in their studies of the impact pressure transients which occur in motor vehicle crashes.

The active material of the transducers is semi-crystalline polyvinylidene fluoride (symbolized by either PVF_2 or PVDF in the polymer literature) which is available in non-piezoelectric sheets. These sheets can be made strongly piezoelectric by first subjecting them to a treatment which enhances the content of one of the crystal forms (a planar zig-zag form referred to as either β-phase or Form I in the polymer literature) and then subjecting them to a poling procedure. For information about the mechanism at the molecular level and about how the piezoelectric activity is affected by sample preparation, treatment, and poling parameters, the reader is referred to a review of the subject [1].

The polymer transducers were developed with two promising applications in mind: 1) the measurement of the normal pressure between two impacting bodies over the interface of contact during impact (this pressure is referred to hereafter as the interface pressure) such as the interface pressure between an anthropomorphic dummy and the instrument panel of a motor vehicle, and 2) the measurement of intracranial pressure in animal subjects, such as rhesus monkeys, during tests of controlled impact to the head.

When mounted to the skin of an anthropomorphic dummy, the thin polymer transducer is not expected to perturb significantly the surface density and mechanical compliance of the dummy. As a result, the interface pressure measured in this application should be representative of the pressure which would occur in the absence of the transducer. When implanted into the cranium of a rhesus monkey, the polymer transducer is expected to move with, rather than relative to, the cranial fluid during impact, because the density of the polymer transducer is comparable to that of the cranial fluid. Thus, in this application too, the pressure measured by the polymer transducer should be representative of the pressure which would occur in the absence of the transducer.

An earlier report [2] covered the development of a polymeric interface-pressure transducer with a circular active area 1 cm in diameter. In this work, it was found that the electrical output of the transducer under general and possibly complicated impact conditions could be explained qualitatively in terms of an output proportional to the pressure normal to the surface of the transducer and an output presumed to depend on membrane strains. The membrane strains may result from bending or stretching of the active area during impact. Measurements described in the earlier report indicated that bending-induced membrane strains could be reduced by lubrication.

The present report covers work performed since the earlier report. This work has proceeded in two main directions, one with the objective of preparing and calibrating 10 intracranial pressure transducers (hereafter referred to as ICPT's) for implantation in rhesus monkeys, and the other with the objective of preparing and calibrating 23 interface-pressure transducers (hereafter referred to as IFPT's) for use on anthropomorphic dummies and other biomechanical subjects.

In the case of the ICPT's, the pressure to be measured is quasi-hydrostatic. Calibration data obtained with a polymer transducer placed in an oil-filled cell and subjected to a known pressure transient have been found to be reproducible to with ± 3%. At NHTSA's request, the ICPT's were made with much-reduced (2-mm diameter)sensitive areas. These small transducers are thus suitable for implantation in the cranium of small lab animals such as rhesus monkeys. Ten or more ICPT's have been calibrated in an oil-filled cell and delivered to NHTSA for use in their other research programs.

A matter which needs to be resolved by further experiments is whether the calibration factor of an ICPT is affected by the thermal conductivity of the fluid into which the transducer is placed. Calculations are given in Appendix B which suggest that the response of a polymer transducer (which is both pyro- and piezoelectric) should contain a significant pyroelectric component associated with adiabatic-compression heating of the transducer under changing pressure. Adiabatic-compression heating of the fluid or other substance in contact with the transducer, if different from that of the transducer, could act as a source or sink of heat for the transducer. Experiments bearing on this matter are suggested in the Recommendations for Future Work at the conclusion of this report.

In the case of IFPT's the pressure to be measured is the normal pressure, that is, the pressure perpendicular to the surface of the transducer. However, the stress induced in the polymer by the impact of compliant bodies may have components parallel to the surface as well. As a result, the response may contain extraneous components. Twenty-three transducers were made with circular active areas 1 cm in diameter and calibrated under transient normal-pressure

conditions while the transducer was sandwiched between a flat-faced, dry, aluminum piston and a dry aluminum disk. These calibration data yielded pressure-response coefficients which are reproducible to within ± 3%. However, the measured coefficients depend on the mechanical and thermal properties of the piston and disk and of any other substance introduced with the sample between the piston and disk. The dry rigid aluminum surfaces of the piston and disk tend to pin the surfaces of the transducer and to keep the temperature of the transducer constant. If the test conditions are changed, the measured coefficients will also change. It has been found, for example, that if the transducer was in frictional contact with compliant instead of rigid surfaces, the output increased by a factor which hereafter will be referred to as the output enhancement,[*] or simply the enhancement. The enhancement depends on the compliance and frictional properties of the impacting bodies. A range of impact situations has been investigated to establish qualitatively the range of variation of the enhancement. Based on these experiments, it is judged that the accuracy with which the effective pressure-response coefficient of a transducer can be predicted for an arbitrary set of field conditions will depend on the accuracy with which the field conditions are known.

Enhancement measurements were also performed on a reduced-area transducer and it was found that the enhancement was vastly reduced. These results suggest that, in the future, reduced-area transducers should be considered not only for intracranial pressure measurements but also for interface-pressure measurements in situations where the enhancement is apt to be large or unpredictable. Still, however, separate calibration methods would be required for each of the two applications. Calibration accuracy for inter-face pressure measurements within ± 10% seems within reach.

*The enhancement is defined arbitrarily as a (multiplicative) factor. The experiments performed in this project can be discussed conveniently using this definition. However, this definition may need revision as more experiments are performed if it turns out that enhancement has additive as well as multi-plicative character.

The fundamental question concerning whether or not mobile real charge (injected during poling as opposed to bound dipolar charge) is present in the polymer is still not resolved and requires future attention. Real charge will contribute to the response if the stress induced across the thickness of the polymer is nonuniform. Nonuniform stresses could be induced in an IFPT during the impact of two bodies which deform differently.

Improvements in Transducer Construction

The polymer transducers delivered to NHTSA since the last report [2] have been improved in the method used to make electrical contact to the miniature electrical connector. Previously, connection from the ground side of the connector to the ground electrode of the polymer was established by a layer of silver-bearing rubber paint in the manner described in Appendix D. Exposure to oil and multiple flexing in time caused this contact to deteriorate and to increase in resistance. This problem has been eliminated by adding a small U-shaped metallic clamp which securely establishes contact with the ground electrode on both sides of the polymer*. A wire connects this clamp to the ground side of the connector. Silver-bearing epoxy is used to further secure the clamp and the whole region, as before, is covered with a coat of silver-bearing rubber paint. The silver- bearing rubber paint, as in the previous design, serves as an extended ground from the miniature electrical connector and thus shields the wire connecting the inner electrodes of the polymer transducer to the center contact of the miniature connector. The external appearance of the transducer is not changed appreciably by this modification.

*The clamp is made from a small (approximately 3 mm x 3mm) piece of brass sheet (100 μm thick) which is bent into a U, and squeezed in a vise until the sides of the U nearly touch. A gap of one-half the thickness of the polymer to be contacted is used.

Reduced-Area Transducer Construction

The construction of the reduced-area transducer is identical to the construction of the transducer with 1-cm diameter active area described previously [2] except that the active area has been reduced from a 1-cm diameter circle to a 2-mm diameter circle, and the electrical improvement discussed in the previous paragraph has been incorporated in the construction.

Figure 1 shows the external appearance of a reduced-area transducer (upper) and a regular transducer (lower). The circular sensitive area in each case appears near the left end.

Oil-Cell Pressure Calibration of ICPT's

A hydraulic transient pressure cell, shown in Figure 2, has been constructed as an accessory to the drop tester. The cell was machined from a massive iron block. During calibration, the polymer transducer is oriented with its active area toward the left end and is attached to a feedthrough electrical connector on the flange shown on the right. A calibrated conventional pressure transducer, which has a pressure-dependent resistance, is mounted through the flange shown on the left with its sensitive face exposed to the pressure inside the cell. The transducer is connected electrically to the mini-box shown in the foreground, which houses a bridge circuit and a battery power supply. The cell is filled with oil and is sealed by means of the piston shown at the top. Pressure transients are generated by impacting the piston. Controlled impact is conveniently achieved by placing the cell in the drop-test machine.

The waveform of the pressure transient is affected by many factors, including air in the oil or in the cell. Air dissolved or entrapped in the oil (which reduces the bulk modulus of the mixture and thus affects the rise time of the
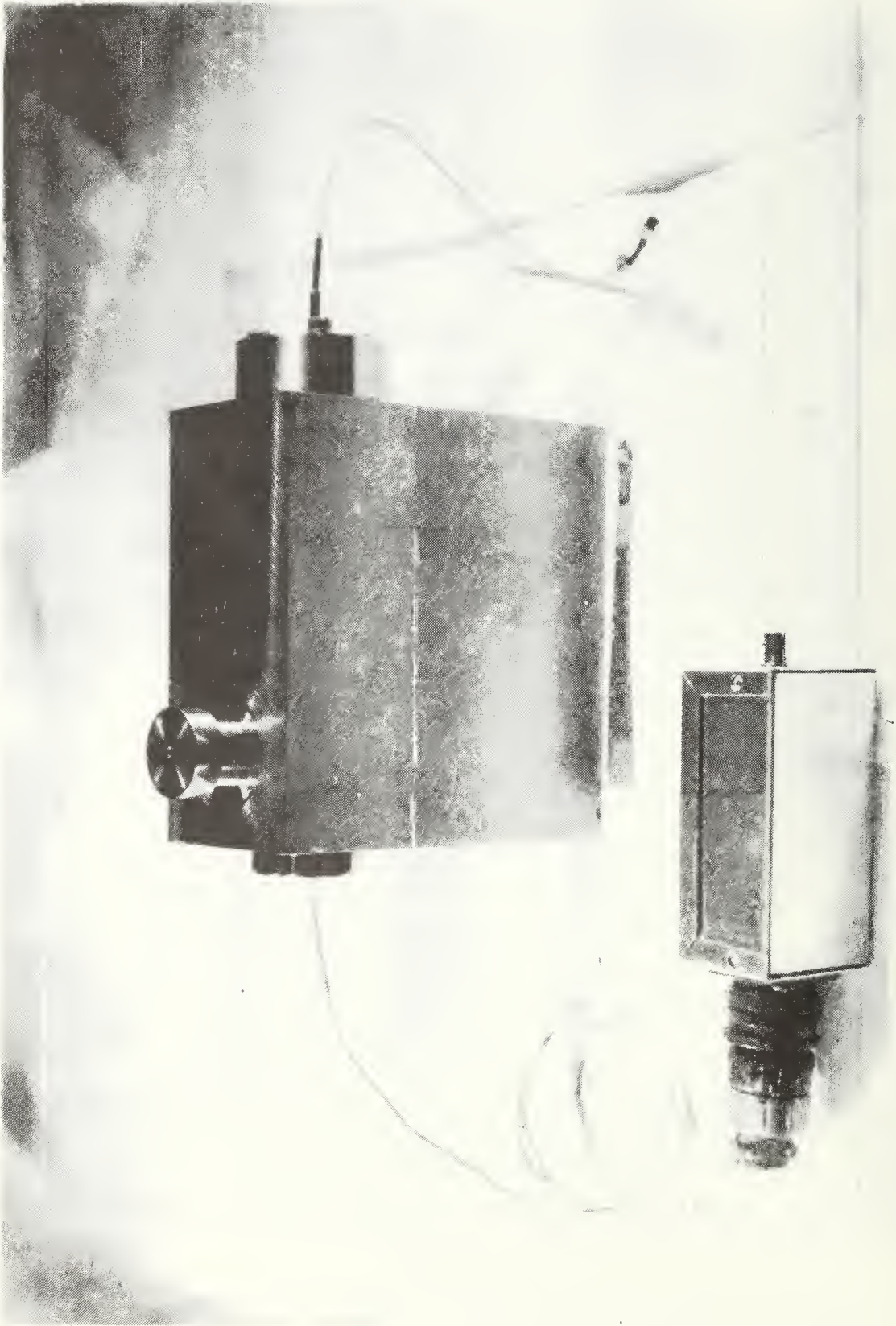
Figure 1: Piezoelectric Polymer Transducers.

Figure 2: Hydraulic transient pressure cell.

pressure transient) can be removed by pumping on the oil under a bell jar until bubbling stops (this requires pumping for a minimum of 15 minutes). Entrapping air in the oil cell during the filling process can be avoided by performing the entire filling operation under vacuum. However, satisfactory filling can be achieved in air using gas-free oil by overfilling the cell to permit the piston to be put in place without trapping air, and then forcing the excess oil through the side flanges. Each flange is loosened in turn while the piston is being depressed. Placing crushable or compliant materials over the piston also affects the waveform. This is a convenient method of shaping the waveform.

The transducer constants (as distinguished from the piezoelectric constants of the polymer material), which are measured during the oil-cell calibration, are either $\Delta Q/\Delta P$ or $\Delta V/\Delta P$, where Q is the charge output measured by a charge amplifier, V is the voltage measured by a high-impedance voltage amplifier, and P is the pressure measured by the calibrated pressure transducer. The force F over the active area of the transducer is $F = PA_a$, where $A_a = (\pi/4) d_a^2$ and d_a is the active diameter, which is found to be greater than the 1-cm electrode diameter. Quantitative information about the effective active area is given in Appendix A.

In terms of the effective piezoelectric constant for a single sheet defined as $d_h \equiv \Delta Q/\Delta F$, the transducer constants are

$$\Delta Q/\Delta P \equiv A_a \ \Delta Q/\Delta F = 2 \ d_h \ A_a,$$

and

$$\Delta V/\Delta P = A_a \ \Delta V/\Delta F = 2 \ d_h \ A_a/C.$$

The subscript h indicates that the constant d_h is measured under quasi-hydrostatic conditions. The factor of 2 comes from the fact that the transducer is bilaminate with two sections electrically connected in parallel so that the respective charge outputs add. The capacitance C includes the capacitance of the active sections, the capacitance of the electrical leads within the transducer and the cable capacitance. If the lead and cable capacitances are negligible, $C \approx 2 \, \varepsilon \, A_a/t$, where ε is the permittivity and t is the thickness of one section of the transducer. An alternate form of $\Delta V/\Delta P$ with C eliminated is

$$\Delta V/\Delta P \approx \frac{d_h}{\varepsilon} t \equiv g_h \, t$$

which is independent of the active area A_a. The constant g_h, appearing above is equal to $(\Delta E/\Delta P)_D$, where E is the induced electric field (E = V/t) and D is the electric displacement. The subscript D means that D is held constant. The area A_a can also be eliminated from the $\Delta Q/\Delta P$ expression, by using the capacitance formula. The expression then becomes

$$\Delta Q/\Delta P \approx C \, t \, g_h \, .$$

For a bilaminate transducer with d_a = 1 cm, t = 25 μm, ε = 10 ε_o where ε_o is the permittivity of free space, the capacitance will be C $\approx$ 1 nF. Using d_h = 10 pC/N, the transducer constants are

$$\Delta Q/\Delta P \approx 2.5 \times 10^{-15} \text{ C/Pa } (17.5 \times 10^{-12} \text{ C/psi})$$

$$\Delta V/\Delta P \approx 2.8 \text{ }\mu\text{V/Pa } (20 \text{ mV/psi})$$

Figure 3 shows an example of the transients measured during calibration using the oil cell. The good correspondence of the transient waveforms produced by the polymer and standard transducers (the latter being known to have a wide frequency response) is indicative of the good frequency response of the polymer transducer in the kHz range. Similar tests using longer and shorter transients indicate similarly good frequency response down to 1 Hz and up to 10^5 Hz.
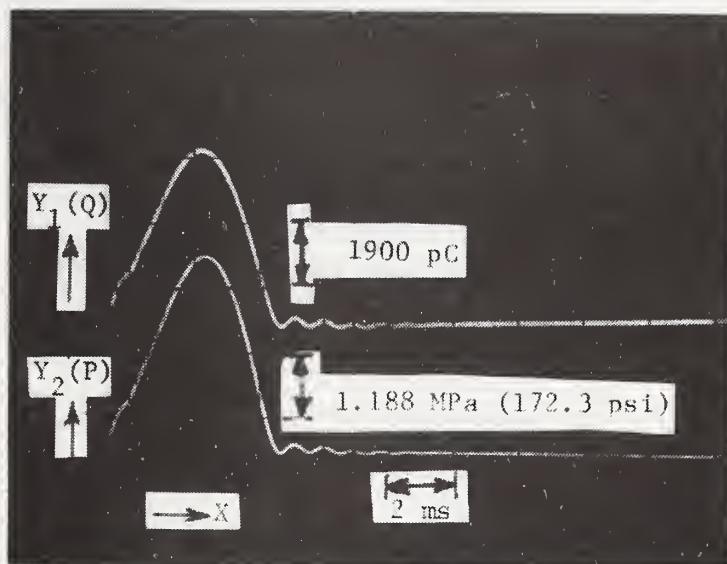
Figure 3. Oscilloscope record of pressure waveform
              obtained in the oil-cell.

Upper trace: Vertical axis $Y_1(Q)$ is proportional to
charge output of polymer transducer.

Lower trace: Vertical axis $Y_2(P)$ is proportional to
voltage output of standard pressure transducer.

Upper and lower trace: Horizontal axis x is propor-
tional to time.

Normal-Impact Pressure Calibration

The fixture shown in the center of Figure 4 was made as an accessory to the drop tester to allow the application of normal pressure transients to the active part of the polymer transducers with 1-cm diameter active areas. The fixture consists of an aluminum piston with flat faces shown toward the top of the fixture. The piston is centered on the fixture and is guided by the fixed bracket, which has a clearance hole for the piston to pass through. A flat disk beneath the piston, which is partly obscured by the polymer transducer, forms the mounting surface for the polymer transducer. In a test, the transducer is inserted between the piston and disk, and the piston is impacted.

The disk is supported rigidly by a calibrated quartz force transducer which is mounted to the disk-shaped base of the fixture. Impact of the piston produces normal pressure transients with a waveform which can be controlled by the placement of a pad beneath the fixture and/or a washer over the piston.

For the reduced-area transducers, the piston is replaced by the assembly shown to the right of the fixture. The lower piece of this assembly serves as a guiding sleeve for the upper piece of this assembly which in turn serves as a reduced-area piston. The diameter of this piston is approximately 2 mm (nominally the same diameter as the active area of the polymer transducer). Thus, the force applied by means of this piston can be confined to the active part of the polymer transducer provided only that the latter is correctly positioned in the test fixture. This arrangement meets the calibration requirement that the force measured by the calibrated force transducer is the force applied to the active area. To interpret the calibration data, it is necessary that the diameter of the piston not exceed the diameter of the active area of the polymer transducer.

Figure 4: Normal-Pressure-Transient Fixture with 1-cm active diameter transducer in place. Assembly at right replaces piston when testing reduced-area transducers.

The transducer constants measured under normal-impact conditions are either $\Delta Q/\Delta F$ or $\Delta V/\Delta F$, where Q is the charge output measured by a charge amplifier, V is the voltage measured by a high-impedance voltage amplifier, and F is the force measured by the force transducer. In terms of the defined piezoelectric constant for a single sheet, $d_n \equiv \Delta Q/\Delta F$, the transducer constants are

$$\Delta Q/\Delta F = 2 \, d_n \,,$$

and

$$\Delta V/\Delta F = 2 \, d_n/C \,,$$

where C is the total capacitance consisting of the transducer capacitance, the cable capacitance and the capacitance of the amplifier-input circuitry. The subscript n indicates that the piezoelectric constant d_n is obtained under normal impact with dry aluminum surfaces contacting the polymer transducer. If d_n = 10 pC/N (44.5 pC/lbf), then $\Delta Q/\Delta F \sim$ 20 pC/N (89 pC/lbf). If C = 1 nF, then $\Delta V/\Delta F \approx$ 20 nV/N (89 mV/lbf).

It should be noted that although d_h (for quasi-hydrostatic pressure conditions) and d_n (for normal pressure conditions) have both been taken as 10 pC/N for the purpose of illustrating the magnitude of the measured transducer constants, they (d_h and d_n) in fact are going to be different by approximately a factor of 2 because the conditions of loading are different. In the case of hydrostatic pressure loading, all the dimensions of the active region are reduced, including the diameter of the sensitive area. In the case of uniaxial loading in the thickness direction, the diameter of the sensitive area will always tend to increase. The increase will be greatest when the transducer is in frictional contact with a high compliance material and smallest when its two surface are perfectly pinned by nearly non-compliant impacting surfaces.

The pressure coefficients are obtained from the force coefficients using the relations,

$$\Delta Q/\Delta P = A_a \ \Delta Q/\Delta F,$$

and

$$\Delta V/\Delta P = A_a \ \Delta V/\Delta F$$

As indicated in the oil-cell calibration discussion, relations exist between the measured transducer constants and the piezoelectric constants of a single polymer sheet. These relations are

$$\Delta Q/\Delta P = 2 \ d_n \ A_a \approx C \ t \ g_n,$$

and

$$\Delta V/\Delta P = 2 \ d_n \ A_a/C \approx g_n \ t.$$

The transducer constants measured by normal impact have been found to be roughly twice as great as those for quasi-hydrostatic loading. Figure 5 shows examples of the transients obtained for normal-pressure calibration.

Output Enhancement Studies

The conditions under which the interface pressure transducers were calibrated were such that the surfaces in contact with the polymer transducer during impact were nearly noncompliant and flat. Thus, to a degree, the active area of the polymer surface was pinned rather than free to slide.

Output enhancement is anticipated if compliant impacting bodies with finite dimensions contact the surfaces of the transducer. The mechanism for this enhancement is believed to be the following. There will be a tendency for compliant material to flow radially outward from the center of impact. A polymer transducer with its center coinciding with the center of impact and its
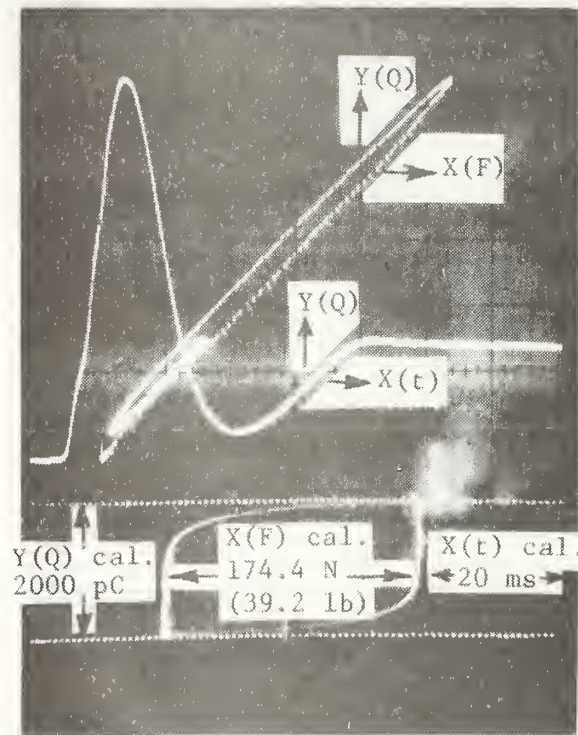
Figure 5: Oscilloscope record obtained with the piston-
impact fixture in Figure 4 fitted with a 1-cm-
diameter polymer transducer. Polymer transducer
was sandwiched between dry aluminum piston above
it and dry aluminum disc beneath it.

Trace Y(Q) versus X(t) is the polymer-transducer
output versus time. Calibration of axes given
as "Y(Q) cal" and "X(t) cal" respectively.

Trace Y(Q) versus X(F) is the polymer-transducer
output versus force-transducer output. Calibra-
tion of X(F) axis is given as "X(F) cal". The mean
slope of Y(Q) versus X(F) gives a polymer trans-
ducer sensitivity of 23.3 pC/N (103.7 pC/lbf).

surfaces in frictional contact with the compliant material will be stretched
radially. The radial stretching, even if slight, may develop sizeable membrane
stresses and, hence, a corresponding component to the transducer response.
This component, not having a simple relationship with normal pressure, is
considered to be extraneous and to constitute a major source of output
enhancement.

While it is possible to reduce this enhancement by lubrication, there are
situations where lubrication may not be desired or practical. For example, there are
instances where it might be desirable to bond a polymer transducer directly to
a compliant body. Thus, it is of interest to find out how much the output
enhancement varies for impact surfaces having a wide range of compliance. It
is also of interest to find out the dependence of the enhancement on the
diameter of the active area of the transducer. Preliminary measurements
described later in this report suggest that the enhancement decreases as the
active area is decreased.

The response Q vs P for each of two transducers having active areas 1 cm
and 2 mm in diameter was measured under each of the following separate test conditions:

a) Dry surfaces of aluminum piston and disk directly in contact with
   polymer transducer surfaces (sandwich structure in the sequence
   Al-IFPT-Al).

b) Oil-lubricated, aluminum piston and disk (Al-oil-IFPT-oil-Al).

c) Polytetrafluoroethylene (PTFE) tape inserted between piston and IFPT
   and disk (Al-PTFE-Poly-PTFE-Al). The thickness of the PTFE tape was
   76 µm (0.003").

d) Unvulcanized rubber sheets inserted between piston and IFPT and between
   IFPT and disk (Al-Rubber-IFPT-Rubber-Al). The thickness of the rubber
   sheet was 760 µm (0.030"). The particular grade of rubber was sticky
   to the touch and adhered to the polymer transducer surfaces after impact.

e)   Rubber sheet as in d) inserted only between piston and IFPT

(Al-Rubber-IFPT-Al).

Configurations b) and c) are believed to approximate field conditions where

a polymer transducer is provided with liquid (oil for instance) or solid

(graphite for instance) lubrication. Configurations d) and e) represent

conditions under which the polymer device is subjected to a considerable amount

of stretch and acts much like a strain gage.

The dry configuration (a), as expected, gave the smallest $\Delta Q/\Delta F$ for both

transducers. For the 1-cm diameter transducer, the oil-lubricated configuration

(b) gave an enhancement of approximately 50% over the dry case, accompanied by

a scatter of $\pm$ 20% in the Q vs F data. The PTFE sandwich configuration (c) gave

an enhancement of approximately 15%. The Q vs F data had little scatter and

were found to remain linear. The rubber-sheet sandwich (d) was found to produce

considerable enhancement and the reproducibility was poor, probably because of

long relaxation times for the viscoelastic rubber material. The enhancement can

be given only roughly as a factor of up to 4 or 5. The configuration with

rubber on one side only (e) also was subject to reproducibility problems. The

enhancement in this case was a factor of around 2.

The above results show that, in order for 1-cm diameter polymer transducers

to yield reliable information about interface pressure, they will have to be

mounted in a manner which avoids or reduces membrane strains. With proper

mounting techniques, it is anticipated that the enhancement should be held within

acceptable limits, and the estimated predictability of the enhancement should

be around $\pm$ 10%. Additional investigative work is indicated in the area of

mounting techniques to insure predictable enhancement for specific field conditions.

The enhancement for the reduced-area transducer was found to be much smaller than that for the 1-cm diameter transducer. The largest enhancement using the configuration Al-Rubber-ICPT-Rubber-Al was found to be only about 40%, a dramatic improvement over the 1-cm diameter transducer. Enhancement is expected to decrease as the radius of the active part of the transducer is decreased. Hence, the reduced-area transducers, which were originally developed for cranial implantation, may be promising interface-pressure transducers for applications where enhancement problems are expected.

Summary of Accomplishments to Date

Since the inception of this two-year project, the following accomplishments have been achieved. 1) Polymer-transducer configurations have been developed for measuring interface pressure and quasi-hydrostatic pressure resulting from impacts. 2) Two transducer versions differing principally in the size of the active area (1-cm and 2-mm diameters respectively) have been evaluated in the laboratory by NBS. The larger size (developed first) was originally intended to measure interface pressure transients, i.e., normal pressure between colliding bodies, and the smaller size (developed later) was intended to measure quasi-hydrostatic pressure transients in the cranial cavity of rhesus monkeys. 3) Normal-pressure test methods have been developed, including a method in which curvature is imparted to the transducer during impact. 4) A quasi-hydrostatic test method has also been developed. The results in the laboratory show promise for the transducers in both types of application. However, used between highly compliant colliding bodies, the transducers, being as thin as they are, are prone to being flexed and stretched, so that outputs not related directly to normal pressure result. It appears that, by devising proper mounting techniques, these

extraneous outputs can be maintained within acceptable limits. However, to
establish this with greater certainty, the transducers need to be tested in
the field with a variety of mounting techniques. 5) It has also been established
in our most recent tests with reduced-area transducers that their extraneous
outputs are much smaller than those of the larger-area transducers. The small-
area transducers should therefore be considered for interface-pressure measurements
in situations where considerable flexing and stretching are anticipated. 6) Twenty-
three (23) transducers with 1-cm diameter active areas were delivered to the
NHTSA as well as ten (10) transducers with 2-mm diameter active areas. These
transducers were tested prior to delivery for ability to withstand pressures of
up to 10^7 Pa (~1000 psi) and were calibrated in the pressure range $0 - 2 \times 10^6$ Pa
(0 - 300 psi) under either normal pressure, quasi-hydrostatic pressure, or both.

Recommendations for Future Work

The work to date has resulted in 1) the development of two versions of
a piezoelectric polymer transducer for two different applications in dynamic
pressure measurements, namely IFPT's for interface-pressure measurements and
ICPT's for intracranial-pressure measurements; 2) the development of test and
calibration methods appropriate for each of the two applications; 3) the
identification of possible physical mechanisms of piezo- and pyroelectric origin
which might give rise to undesirable components in the transducer response; and
4) the delivery to NHTSA of the contract-specified numbers of calibrated IFPT's
and ICPT's.

Because of the restricted scope of the work to date, several aspects of
the behavior of polymeric pressure transducers have been left in a preliminary
stage of investigation. This fact and the fact that the range of impact con-
ditions (dynamic stresses other than normal pressure and dynamic temperature
excursions) which are likely to be met in practice are not clearly established,
suggest that further progress will be made most efficiently through the close
coordination of laboratory and field work. The laboratory work is to gain a
greater understanding of the spurious outputs due to both piezo- and pyroelectric
effects. The field work is to obtain a realistic knowledge about the range of
stress and temperature excursions over the considerable variety of foreseeable
field applications, and to identify specific problem areas the knowledge of which
can guide the laboratory work. Deficiencies in performance in a given field
application do not necessarily indicate an inherently fatal property of polymeric
transducers, but merely a weakness of one particular transducer design for that
specific application to be corrected by further development.

The following work is recommended with the broad aim in mind of arriving at a pressure transducer with properties so well known that it can be used effectively by any technically competent personnel provided only that they consult the calibration report and follow simple, recommended mounting practices:

1) To minimize the spurious response of an IFPT due to stretching and flexing relative to the response due to normal pressure, the diameter of the active area should be made as small as is practical. Experiments described in the Enhancement Studies section of this report have shown that the enhancement of a 2 mm diameter transducer is smaller than that of a 1 cm diameter transducer. The theory in Appendix C indicates that stretching effects under spherical impacts can also be minimized by reducing the active area. The diameter cannot be reduced indefinitely, however, as the voltage sensitivity, low-frequency response and noise figure will be degraded if the capacitance of the active region becomes comparable to or smaller than the capacitance of the electrical leads and shunt capacitance of the amplifier input. The optimum transducer size should be determined by performing a study of the dependence of the enhancement on the radius of the transducer active area under controlled laboratory impact conditions. This study would require constructing several transducers with the same thickness but with different active areas.

2) To gain the benefits of reduced active area without prohibitive loss of capacitance, an IFPT could be constructed with several small mechanically isolated, but electrically connected active areas. Mechanical isolation could be achieved by making the active regions stiff and resistant to stretching compared with the intervening inert regions.

3) Special transducer configurations for special applications should also be investigated. For example, a ring or washer-stabilized prestressed membrane configuration may reduce the effects of membrane strains in situations where the membrane remains plane.

4) To compensate both IFPT's and ICPT's for pyroelectric response, the dynamic temperature change experienced by the active areas should be determined under representative pressure-measuring conditions. These temperature transients could be obtained by measuring the temperature-dependent resistance change of one of the thin-film electrodes, or by measuring the thermoelectric voltage of a thin-film thermocouple deposited on one of the electrodes.

5) The change in pressure sensitivity due to changes in ambient temperature should be measured over a range of temperature spanning the extremes anticipated in the field.

6) A field calibrator should be designed, built, calibrated, and field tested. Such an instrument could measure the in-situ response of an IFPT to a pressure transient produced by the calibrator. Many of the spurious effects would thus be automatically compensated for, including those induced by variations of mounting technique and those induced by variations of local conditions.

7) It would be of interest also to measure the effects of the response of changing dynamically the surface charge on the external surfaces of the transducer. The motivation for this measurement is that there are plans to measure seat-belt pressures against a restrained body. Seat-belt materials could be triboelectric which could result in significant charging of the material in contact with the polymer transducer.

Appendix A. Effective Active Area

The effective active area of a polymer transducer of the type described in this report appears to be somewhat greater than the area of the poling electrodes. This can be demonstrated by measuring the piezoelectric response of a transducer to piston pressure, as the piston radius, r, is varied over a range of values including values in excess of the electrode radius, r_e.

For $r \leq r_e$, the short-circuit charge output Q produced by force F, is given by $Q(r < r_e) = 2\ d_n F$, which is independent of r. For $r > r_e$ the charge output with the assumption that the active area is limited to the electrode area is given by $Q(r > r_e) = 2\ d_n F(\frac{r_e}{r})^2$, a decreasing function of r with maximum negative slope at $r = r_e$. Thus, a sharp break in the r-dependence is predicted at $r = r_e$.

Table 1 shows the results of a set of measurements performed on a typical transducer, for which $r_e = 1$ cm, for six pistons of different radii, together with corresponding theoretical predictions for comparison. The results bear out the predicted independence on r, for $r < r_e$, but do not indicate a sharp decrease in response starting at $r = r_e$. Instead, the sharp decrease begins around $r = 1.2\ r_e$ suggesting that the effective piezoelectrically active area extends radially approximately 20% beyond the electrode boundary.

The origin of the extended active area has not been established. However, several factors could contribute. During poling, the poling voltage may extend beyond the poling electrode boundary due to electrical breakdown of the air or to charge leakage along the surface. Electrical fringe effects and real-charge

Table 1

Variation of Transducer Response with Piston Radius

r_e (electrode radius)	r (piston radius)	Theory[1]	Experiment[2]
1 cm	0.8 cm	1.0	1.06
	0.9 cm	1.0	0.94
	1.0	1.0	–
	1.1	0.83	1.07
	1.2	0.69	0.92
	1.3	0.59	0.63
	1.4	0.51	0.49

(1) This column lists normalized response $Q(r)/Q(r<r_e)$ where $Q(r<r_e) = 2d_n F$ for $r<r_e$, and $Q(r) = 2d_n F r_e^2/r^2$ for $r>r_e$.

(2) This column lists $Q(r)/Q(r<r_e)$ when $Q(r<r_e)$ was taken as the mean of 4 high readings.

injection will further influence the poling field distribution. Finally, during piezoelectric response measurements, mechanical fringe effects giving rise to inhomogeneous stresses around the edge of the piston can introduce a real-charge component to the response. This component will be greatest when $r \approx r_e$, in which case the mechanical fringe volume coincides with the electrical fringe volume.

The effects of extended active area on the accuracy of the device calibration and on the reliability of using laboratory calibration data in field measurements have not been quantitatively established. The importance of these effects, however, is expected to increase as the radius of the transducer is decreased. Thus, there may be cause for concern in the case of reduced-area transducers. One way to eliminate extended active area would be to make transducers with active sections cut out of larger poled sheets. This procedure, however, increases the complexity of the device construction.

Appendix B.   Effects of Heating under Adiabatic Compression

The piezoelectric polymer transducers discussed herein are also pyroelectric. The pyroelectric coefficient is in the neighborhood of 4 $nC \cdot cm^{-2} \cdot K^{-1}$, yielding an open-circuit voltage response of 6.3 V/K for a 1-cm diameter bilaminate device with 1 nF capacitance. At low frequencies, a transducer in good thermal contact with a metallic base plate will respond nearly isothermally. At high frequencies the same transducer will respond nearly adiabatically. This appendix suggests that the difference between the isothermal and adiabatic response is significant because plastics heat up sufficiently during adiabatic compression.

The thermodynamic relation for the pressure-induced infinitesimal temperature change under adiabatic compression is

$$\frac{dT}{dP} = \frac{T \beta_p v}{C_p} ,$$

where T is the temperature, P is the pressure, v is the specific volume β_p is the thermal expansion coefficient at constant pressure $\frac{1}{v} (\frac{\partial v}{\partial T})_p$, and C_p is the specific heat at constant pressure.

At T = 300 K, we have $C_p \approx 1.3$ J g^{-1} K^{-1}, v = 0.6 x 10^{-3} $\frac{m^3}{Kg}$ and $\beta_p \approx 3$ x 10^{-4} K^{-1} for polyvinylidene fluoride. These data give

$$\frac{dT}{dP} \sim 4.2 \text{ x } 10^{-8} \text{ K/Pa } (0.3 \text{ x } 10^{-3} \text{ K/psi})$$

The pyroelectric responsivity due to adiabatic compression heating is thus predicted to be 0.26 μV/Pa (1.8 x 10^{-3} V/psi). This is about 17% of the piezoelectric responsivity under hydraulic pressure which is around 1.5 μV/Pa (10 mV/psi), and is of opposite sign.

The above analysis suggests three possible environmental situations.

Case 1:   dT/dP of surroundings is the same as dT/dP of the polymer transducer.   The transducer exchanges no heat with its surroundings and its response is adiabatic at all frequencies.

Case 2:   dT/dP = 0 for surroundings and surroundings act as a constant temperature bath.   The transducer exchanges heat with its surroundings with a characteristic equilibration time τ.   Its response will be adiabatic at high frequencies compared to $1/\tau$ and isothermal at low frequencies compared to $1/\tau$.   At intermediate frequencies, the frequency response should exhibit a smooth decrease with increasing frequency corresponding to a change from isothermal to adiabatic conditions.

Case 3:   dT/dP of surroundings is much greater than dT/dP of polymer. In this case, the response at low frequencies compared to $1/\tau$ will be dominated by the pyroelectric effect, while the response at high frequencies compared to $1/\tau$ will be adiabatic.

Appendix C. Response due to Stretching Resulting from Impact by a Sphere

Consider a polymeric transducer with an active surface of radius r_o, which is mounted on an initially flat, yielding material such as a foam-rubber pad. The transducer and the pad are impacted at normal incidence by a spherical, rigid object of radius R, where $R > r_o$. Contact between impactor and transducer occurs first at the center of the transducer. The impactor indents the pad to the extent that the initially plane surface of the transducer is forced to conform to the shape of the spherical impactor. After the transducer has fully conformed to the shape of the impactor, the impactor continues to indent the pad, and the deforming pad causes the transducer to stretch further while sliding over the surface of the impactor. The membrane-extensional response of the transducer (short-circuit charge or open-circuit voltage), can be considered an "error" response. For the purposes of computing this error response, assume that the membrane-extensional deformation of the transducer proceeds in two stages.

During the first stage, assume that the planar surface of the transducer transforms into a spherical cap by orthographic projection (refer to Fig. 6). Imagine a polar grid pattern printed on the active surface of the transducer. Before deformation, the pattern which has its pole at the center, consists of concentric circles centered on the pole which are intersected by lines radiating from the pole. In the assumed deformation process, the circles map into latitude circles without change in radius, while the radial lines map into meridians with an increase in length. The membrane deformation is thus considered to be purely radial in this stage.
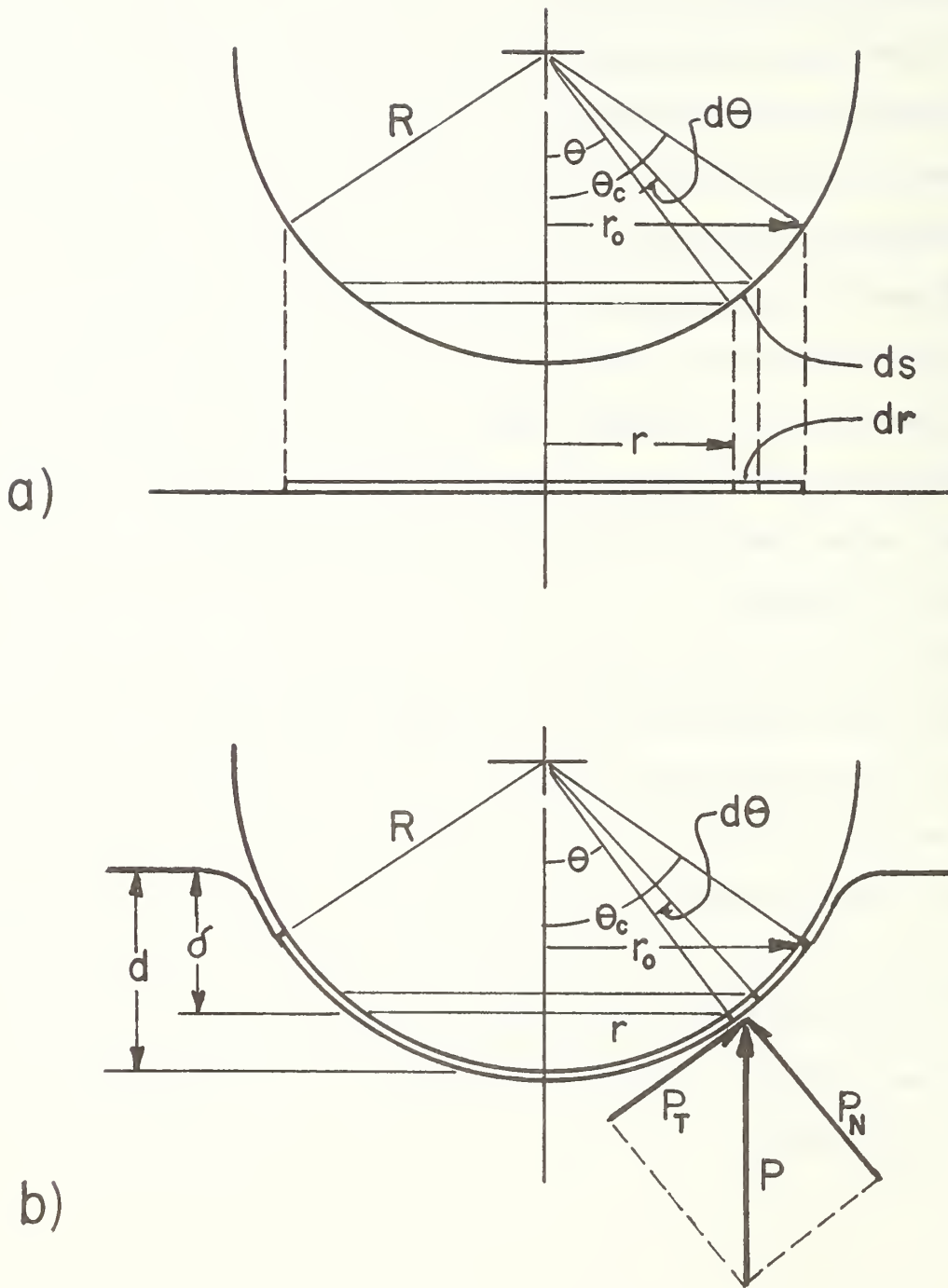
Figure 6. Impact of rigid sphere and initially flat, semi-infinite, compliant pad with circular (thin sheet) polymeric transducer on its surface: a) before impact; b) at the end of the first stage of indentation when the transducer has fully conformed to the shape of the impactor.

The piezoelectric equation which applies [3] during the first stage, is

$$E_3^D = \frac{V}{t} = - h_{3r} \, S_r, \text{ for } D = 0 \tag{1}$$

where E_3^D = the electric field across the thickness of the polymer sheet under conditions of constant electric displacement D.

V = the corresponding open-circuit voltage output.

t = the thickness of the polymer sheet.

h_{3r} = the piezoelectric constant relating the appropriate component of field across the thickness to radial strain.

S_r = the radial strain.

Referring to Fig. 6 (a), the radial differential element, dr, transforms into the differential arc length ds = R dθ. The strain at a general radius r is thus

$$S_r = \frac{ds - dr}{dr} = \frac{R \, d\theta}{dr} - 1 = \frac{1}{\cos \theta} - 1 = \frac{1}{\sqrt{1 - (\frac{r}{R})^2}} - 1. \tag{2}$$

The field at r is, according to Equation (1):

$$E_3(r) = h_{3r} \, [\frac{1}{\sqrt{1 - (\frac{r}{R})^2}} - 1]. \tag{3}$$

The charge induced on the electrodes of the transducer is, by Gauss's law:

$$Q = \int_A \varepsilon \, E_3 \, dA, \tag{4}$$

where ε is the dielectric permittivity of the polymer sheet (typically, $\varepsilon \approx 10 \, \varepsilon_o$, where ε_o is the permittivity of free space), E_3 is the position-dependent field in Equation (3) and dA is the differential element of area with circumference $2\pi r$ and width $ds = R \, d\theta = \frac{dr}{\cos \theta} = \frac{dr}{\sqrt{1 - (\frac{r}{R})^2}}$. The integration gives

$$Q = 2\pi \varepsilon h_{3r} \int_0^{r_o} \left[\frac{1}{\sqrt{1 - (\frac{r}{R})^2}} - 1\right] \frac{rdr}{\sqrt{1 - (\frac{r}{R})^2}} \tag{5}$$

$$= 2\pi \varepsilon h_{3r} R^2 \left\{-\frac{1}{2} \ln\left[1 - (\frac{r_o}{R})^2\right] + \sqrt{\frac{r_o^2}{1 - (\frac{r_o}{R})}} - 1\right\}. \tag{6}$$

The open-circuit voltage is $V = Q/C$, where C is the strain-dependent capacitance. If, for simplicity, it is assumed that the deformation conserves polymer volume, and that ε is independent of strain, then $C = \dfrac{\varepsilon A}{t} = \dfrac{\varepsilon \pi r_o^2}{t}$ will not depend on strain. In that case, the effect on the capacitance of increased area is compensated exactly by the effect of decreased thickness.

Result (6) can be condensed if $r_o/R \ll 1$ by approximating $\ln\left[1 - (\frac{r_o}{R})^2\right]$ and $\sqrt{1 - (\frac{r_o}{R})^2}$ by the leading terms of their respective series expansions to obtain

$$Q = \frac{3\pi \varepsilon h_{3r}}{4} R^2 (\frac{r_o}{R}). \tag{7}$$

The voltage for polymer volume-conserving strains and constant ε is

$$V = Q/C = 3/4\, h_{3r}\, t\, \frac{r}{R}. \tag{8}$$

This voltage is seen to depend on r. Thus, for a given R and t, V can be reduced by reducing r.

During the second stage, the deformation is more complicated. If the transducer surfaces were ideally lubricated, then this deformation would be zero. If the transducer can slide freely over the surface of the impactor but cannot slide relative to the pad, then the pad deformation will cause the grid pattern to expand in area. In that case, both the latitude circles and meridians will stretch.

The error voltage in this stage is probably going to depend on F_T the integral of the tangential component of the pad reaction pressure P over the transducer surface. The evaluation of the integral requires a knowledge of the tangential pressure distribution P_T (θ) or some assumption to be made about its form.

The integral is straightforward if the pad reaction pressure over the contact interface is assumed to be directed oppositely to the motion of the impactor as shown in Fig. 6(b) and if the pressure is assumed to be either constant or linearly dependent on the indentation. The area element is dA = 2π R^2 sin θ dθ.

Under the constant-pressure asumption, the integral is

$$F_T = 2\pi P R^2 \int_0^{\theta_c} \sin^2 \theta \, d\theta$$

$$= 2\pi R^2 P [\frac{\theta_c}{2} - \frac{1}{4} \sin 2\theta_c],$$

where θ_c is the half-angle subtended by the contact interface.

Under the assumption that the local pressure, P, and the local indentation, δ = d − R (1 − cos θ), are linearly related, i.e. P = kδ, the integral is

$$F_T = 2\pi R^2 k (d - R) \int_0^{\theta_c} \sin^2 \theta \, d\theta$$

$$+ 2\pi R^3 k \int_0^{\theta_c} \sin^2 \theta \cos \theta \, d\theta$$

$$= 2\pi R^2 k (d - R) (\frac{\theta_c}{2} - \frac{\sin 2\theta_c}{4}) + \frac{2\pi}{3} R^3 k \sin^3 \theta_c.$$

Under either assumption, F_T is seen to increase with θ_c. This suggests that the error voltage in the second stage of deformation, as in the first stage, can be reduced by reducing the radius of the transducer.

Appendix D. Details of Transducer Construction

This appendix is a reproduction of Section 3.2 of the earlier report (NBSIR 75-740) which gave details of the construction of 1-cm-diameter transducers. The procedure produces bilaminate transducers in lots of nine.

(1) Two rectangular sheets, 13 cm x 16 cm, are cut from a roll of capacitor-grade PVF_2 sheet 25-μm thick.

(2) Each sheet of PVF_2 is sandwiched between two sheets of glass. This assembly is placed in an oven and is heat-treated at 130 ± 10°C for approximately two hours. This annealing treatment serves to reduce permanent and severe dimensional changes during subsequent steps.

(3) On one side of each sheet (referred to as the electrical high side) a mask-defined pattern of nine identical aluminum electrodes, as shown in Fig. 7, is deposited by evaporation in a vacuum chamber. The pattern is defined by an evaporation mask which is also shown in Fig. 7. Aluminum was selected as the electrode material because it is easy to evaporate, adheres well to the polymer substrate, and has good electrical conductivity in thin-film form. Each electrode consists of a 1-cm-diameter circular area connected to a 0.2-cm-diameter circular dot by a strip 10.1-cm long and 0.04-cm wide. The 1-cm-diameter spot defines the area which ultimately becomes active; the strip serves as an electrical lead, and the small dot as a pad for later electrical connection to the center conductor of a low-noise cable. The nine electrodes are deposited side-by-side, so that the nine strip leads are parallel and 1.6-cm apart, while the 1-cm-diameter spots and and the 0.2-cm-diameter pads form respective parallel linear arrays, nominally 10 cm from each other. Approximately 0.2 μm of aluminum is deposited, which results in a strip lead resistance of less than 100 Ω.
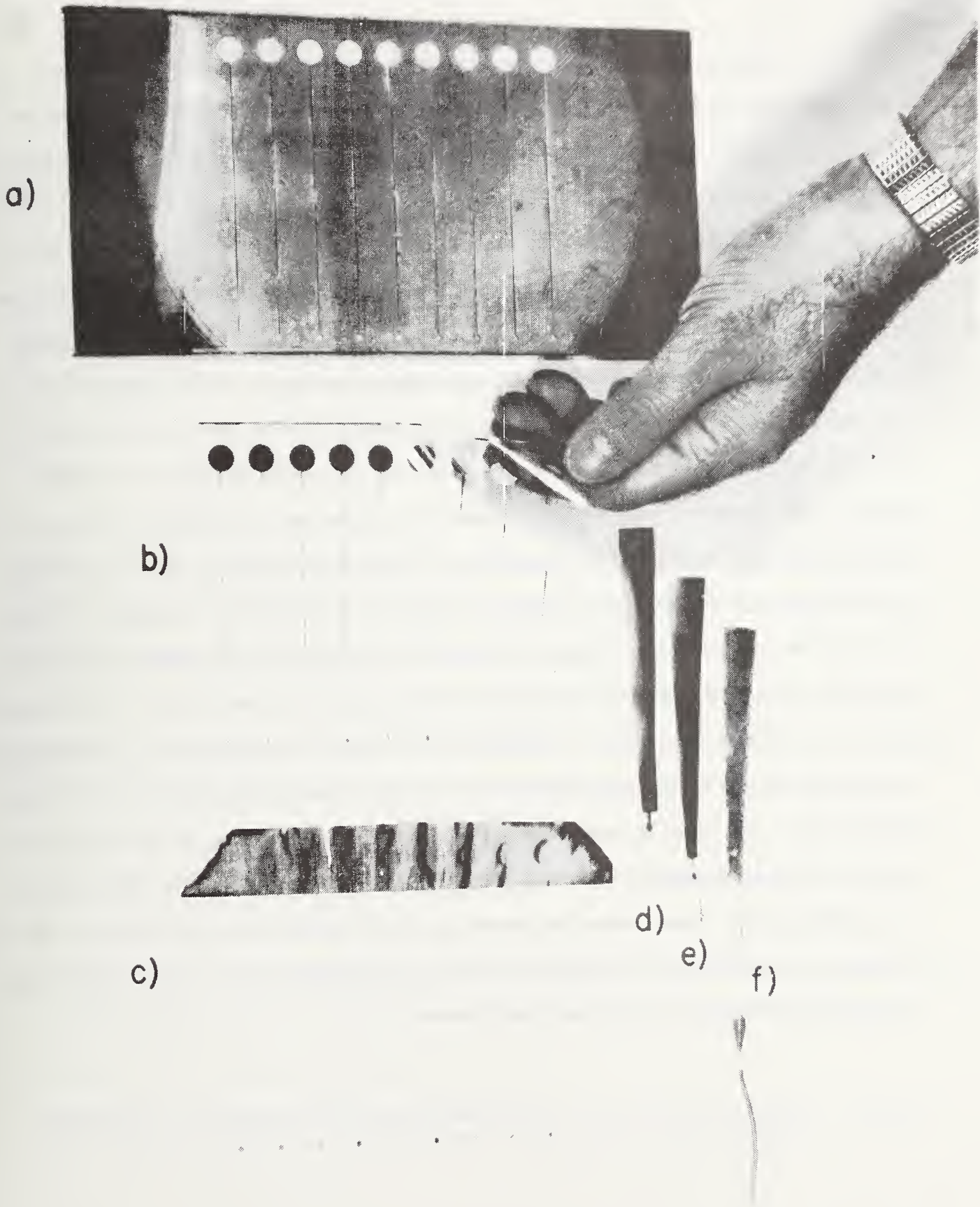
Figure 7.   a) Mask. b) PVF$_2$ sheet after deposition of positive (high) electrodes. c) PVF$_2$ sheet after deposition of negative (low) ground strip and ready for poling. d) Bilaminate transducer after wire bonding. e) Bilaminate transducer after positive electrode is connected to miniature connector. f) Finished transducer and mating coaxial cable.

(4) On the opposite side of each sheet a strip electrode, 3-cm wide and approximately 0.1-μm thick, is deposited in line with the array of 1-cm-diameter dots. During poling, this strip serves as a common electrical ground electrode. Fig. 7 shows how this strip is oriented.

(5) Each sheet, together with two strips of tin foil for electrical contact to the exterior, is then sandwiched between two insulating sheets of 250-μm-thick polyethylene terephtalate. One tin-foil strip contacts the common ground electrode, and the other contacts all nine high-side leads. This assembly is mounted between the 23 x 23-cm platens of a hydraulic hot press, and a load of approximately 40 kN (four-tonf gage reading) is applied. The positive output terminal of a high-voltage d-c power supply is connected to the high electrode, and the negative terminal is connected to the ground electrode. The steel frame of the press and the negative terminal of the power supply are connected to laboratory ground. A poling voltage of 2000 $\pm$50 V is applied, corresponding to a field of about 8×10^5 V/cm across the polymer in the region defined by the 1-cm-diameter areas. The PVF_2 is heated to a temperature of 120°C, as measured by a thermocouple inserted between the insulating sheets, and cooled immediately thereafter to room temperature. The heating part of the cycle takes approximately 20 min. and the cooling part approximately 15 min. This procedure poles the PVF_2 selectively in the regions of the 1-cm areas, and leaves the nine strip-leads effectively inactive. Pressure is applied during poling to prevent wrinkling of the polymer sheets under the combined effects of field and temperature.

(6) After removal from the press, an aluminum shield electrode, 0.1-μm thick, is deposited on the ground side of each sheet, extending the ground electrode to cover nominally the entire surface of that side of the sheet. To avoid depoling the nine activated areas during this evaporation, which heats the polymer substrate, the part of the ground electrode used during poling consisting of a 1.5-cm-wide strip opposite the set of 1-cm-diameter dots, and aligned with them, is masked off by a metal strip. Another strip, also 1.5-cm wide, masks off another area, opposite the set of 0.2-cm-diameter dots on which it is centered to provide a clear area for visual alignment of one sheet with another in a later step.

(7) The high side of each sheet is then coated with a thin layer of contact cement[*] by wiping the surface with a foam-rubber pad saturated with a solution of contact cement diluted 5 to 1 with toluene. The contact cement is allowed to dry at least 15 min. to allow the solvent to evaporate.

(8) Nine pieces of 250-μm-diameter, tinned-copper wire are cut to a length of 5 cm, and one end is flattened over a length of approximately 0.6 cm, by rolling the end in a bench-type rolling mill. The flattened portions of the nine wires are coated with a thin layer of silver-bearing epoxy and are laid on the nine high leads of one of the sheets, in a manner such that the flattened portion contacts the 0.2-cm-diameter dots at the ends of the evaporated leads. A small drop of contact cement is then applied to each wire immediately behind the flattened portion to form a fillet for the round wire and to hold the wire in place on the sheet.

---

[*] Considerable experimentation was conducted with various bonding agents. Contact cement meeting Federal Specification MMM-A-130a has been satisfactory.

(9) The two sheets are precisely positioned on separate, mating, vacuum-hold-down plates with the high, cement-coated, sides facing out. At the same time, they are stretched lightly to make them lie as flat as possible. The plates are then mated so that the cement-coated sides are pressed together to form a bilaminate assembly. Care must be exercised prior to and during this step to insure that when the sheets are bonded, the pattern of dots and leads on one sheet is in satisfactory alignment with the corresponding pattern on the other sheet, and that trapping of air bubbles is minimized. The assembly is then placed in the hydraulic press and further pressed under a load of approximately 250 kN (25-tonf gage reading).

(10) The bonded sheets are then cut to yield nine separate bilaminate transducer elements. A 12-μm layer of unpoled PVF_2 is then cemented on each side of the elements, covering all but the small portion of the shield electrode at the end where electrical contact is to be made. These layers act as a protective coating to prevent damage to the shield electrode.

(11) The wire lead of each element is trimmed to leave approximately 0.3 cm protruding outside the polymer sheets. This lead is then soldered to the center conductor of a female miniature bulkhead coaxial connector. Care is taken not to damage the connection to the evaporated lead by excessive soldering heat conducted by the wire.

(12) The exposed parts of the high lead between the connector and the end of the transducer not covered by the shield electrode are potted in epoxy. After the epoxy has hardened, electrical contact between the shield side of the transducer is made by applying a thick coat of liquid, silver-bearing rubber, over the insulating epoxy and the area surrounding it.

Bibliography

[1]   M. G. Broadhurst and G. T. Davis, Piezo- and Pyroelectric Properties
      of Electrets, NBSIR 75-787, October 1975.

[2]   A. S. DeReggi, Piezoelectric Polymer Transducer for Impact Pressure
      Measurement, NBSIR 75-740, July 1975.

[3]   D. A. Berlincourt, D. R. Curran, and H. Jaffe in Physical Acoustics,
      W. P. Mason, Ed. (Academic, New York, 1964) 1, Part A., Chapter 3, p.188.

U.S. DEPT. OF COMM. **BIBLIOGRAPHIC DATA SHEET**	1. PUBLICATION OR REPORT NO. NBSIR 76-1078	2. Gov't Accession No.	3. Recipient's Accession No.
4. TITLE AND SUBTITLE Piezoelectric Polymer Transducers for Dynamic Pressure Measurements		5. Publication Date	
		6. Performing Organization Code	
7. AUTHOR(S) A. S. DeReggi, S. Edelman, S.C. Roth		8. Performing Organ. Report No.	
9. PERFORMING ORGANIZATION NAME AND ADDRESS NATIONAL BUREAU OF STANDARDS DEPARTMENT OF COMMERCE WASHINGTON, D.C. 20234		10. Project/Task/Work Unit No.	
		11. Contract/Grant No.	
12. Sponsoring Organization Name and Complete Address (Street, City, State, ZIP) National Highway Traffic Safety Administration Department of Transportation NASSIF Building Washington, D.C. 20590		13. Type of Report & Period Covered Final	
		14. Sponsoring Agency Code	

15. SUPPLEMENTARY NOTES

16. ABSTRACT *(A 200-word or less factual summary of most significant information. If document includes a significant bibliography or literature survey, mention it here.)*

    This report describes the construction, testing and calibration of piezoelectric polymer sensing transducers of two sizes. The piezoelectric material was obtained by poling 25 µm thick, polyvinylidene fluoride sheet. Sensors with an active area of 1 cm diameter, intended for dynamic interface-pressure measurements, were calibrated in a fixture generating normal pressure transients by means of piston impact. Sensors with an active area of 2 mm diameter, intended for measuring dynamic pressures while implanted in the cranium of rhesus monkeys, were calibrated in an oil cell with a piston-cylinder seal which provided hydraulic pressure transients by means of impact on the piston. The larger sensors had a normal-pressure sensitivity around 3 µV/Pa (20 mV/psi) and the smaller sensors a hydraulic-pressure sensitivity around 0.7 µV/Pa (5 mV/psi).

17. KEY WORDS *(six to twelve entries; alphabetical order; capitalize only the first letter of the first key word unless a proper name; separated by semicolons)* Piezoelectric; polymer; polyvinylidene fluoride; pressure sensor; pyroelectric; transducer

18. AVAILABILITY [X] Unlimited	19. SECURITY CLASS (THIS REPORT) UNCLASSIFIED	21. NO. OF PAGES 41
☐ For Official Distribution. Do Not Release to NTIS		
☐ Order From Sup. of Doc., U.S. Government Printing Office Washington, D.C. 20402, SD Cat. No. C13	20. SECURITY CLASS (THIS PAGE)	22. Price
[X] Order From National Technical Information Service (NTIS) Springfield, Virginia 22151	UNCLASSIFIED	$4.00